

## Original Investigation

# Carotid Plaque-RADS Score Combined with Pericarotid Fat Density—An Incremental Prediction Model for Stroke Recurrence

Jinhua Qian,<sup>1</sup> Qinjie Chi,<sup>1</sup> Li Zhu, Tianhao Zhang, Wenbing Ding, Ruifan Yuan, Zhuo Chen, Tianle Wang

**Rationale and Objectives:** This study aimed to evaluate the prognostic value of combined carotid plaque reporting and data system (RADS) score and pericarotid fat density (PFD) for predicting stroke recurrence risk, and to explore its utility in stroke risk stratification.

**Methods:** We developed a novel binary comprehensive risk index (CRI) that integrates the carotid plaque-RADS and PFD: low CRI (RADS < 3 and PFD ≤ -74 HU) and high CRI (RADS ≥ 3 or PFD > -74 HU). Net reclassification improvement, Kaplan–Meier survival analysis, multivariate logistic regression, receiver operating characteristic curves (ROC), and decision curve analysis (DCA) were used to assess the predictive value of CRI over stenosis degree.

**Results:** During a mean follow-up period of 17.24 ± 11.93 months, 64 of 272 patients (23.3%) experienced recurrent stroke. CRI significantly improved stroke recurrence risk stratification in mild-to-moderate stenosis patients. Kaplan–Meier survival analysis revealed significant differences in stroke recurrence rates across varying plaque-RADS and CRI ( $P < 0.0001$ ). Independent predictors of stroke recurrence included plaque-RADS ≥ 3 (OR = 2.68, 95% CI: 1.03–6.96), CRI (OR = 8.25, 95% CI: 2.23–30.44), affected-side PFD (OR = 0.97, 95% CI: 0.94–0.99), and bilateral PFD difference (OR = 1.09, 95% CI: 1.05–1.13). The combined model incorporating stenosis degree, plaque-RADS, affected-side PFD, bilateral PFD difference, and CRI demonstrated superior prediction performance, achieving an area under the ROC curve of 0.892.

**Conclusion:** Integrating carotid plaque-RADS and PFD significantly enhances the accuracy of stroke recurrence risk prediction, especially in patients with mild-to-moderate stenosis. This combined assessment model provides valuable insights for personalized prevention and treatment strategies for stroke recurrence.

**Key Words:** Carotid plaque; Carotid plaque-RADS; Pericarotid fat density; Recurrent stroke; Stroke.

© 2025 The Association of Academic Radiology. Published by Elsevier Inc. All rights are reserved, including those for text and data mining, AI training, and similar technologies.

**Abbreviations:** RADS reporting and data system, PDF pericarotid fat density, CRI comprehensive risk index, HU hounsfield unit, ROC receiver operating characteristic curves, DCA decision curve analysis, IPH intraplaque hemorrhage, FC fibrous cap, CTA computed tomography angiography, HR-VWI high resolution-vessel wall imaging, MWT maximum wall thickness, NRI net reclassification index, AUC area under the curve

Acad Radiol xxxx; xx:xxx-xxx

From the Department of Radiology, Affiliated Hospital 2 of Nantong University, Nantong 226600, China; Department of Intervention, Affiliated Hospital 2 of Nantong University, Nantong 226600, China; Department of Neurology, Affiliated Hospital 2 of Nantong University, Nantong 226600, China. Received March 20, 2025; revised April 18, 2025; accepted April 21, 2025. Address correspondence to: T.W. e-mail: wangtianle9192@163.com

<sup>1</sup> Jinhua Qian and Qinjie Chi contributed equally as first authors

© 2025 The Association of Academic Radiology. Published by Elsevier Inc. All rights are reserved, including those for text and data mining, AI training, and similar technologies.

<https://doi.org/10.1016/j.acra.2025.04.051>

## INTRODUCTION

Stroke is the second leading cause of death worldwide, with ischemic strokes accounting for approximately 85% (1). Despite significant advancements in treatment and secondary prevention strategies, the risk of recurrence remains substantial after an initial stroke. Systematic reviews and meta-analyses indicate that the recurrence rate is 11.1% within the first year post-stroke and ranges from 20% to 30% within five years (2,3). Notably, patients with large-artery atherosclerotic stroke exhibit significantly higher recurrence rates than those with other etiologies (4). The carotid artery, a major extracranial vessel, is frequently affected by large-artery atherosclerotic

lesions. Atherosclerotic plaque formation and progression in the carotid artery directly impact cerebral blood supply, accounting for approximately 20% of all strokes (5). Given the critical role of carotid plaques in both the onset and recurrence of ischemic stroke, accurately identifying and classifying high-risk plaques for stroke recurrence is of paramount importance.

Traditional assessments of stenosis severity, such as the North American Symptomatic Carotid Endarterectomy Trial criteria, are linked to an increased risk of recurrent stroke, yet their predictive power remains insufficient, particularly in patients with mild-to-moderate stenosis (4). Carotid atherosclerosis is a complex process influenced not only by stenosis severity but also by plaque vulnerability (6). Beyond structural assessment, inflammation plays a crucial role in atherosclerosis progression, influencing plaque stability and the risk of cerebrovascular events (7–9). These findings underscore the need for a more comprehensive stroke risk assessment that goes beyond stenosis degree to include both plaque vulnerability and inflammation.

In recent years, the Carotid Plaque-RADS and PFD have emerged as advanced imaging tools with the potential to enhance stroke recurrence risk prediction. In the 1990s, the American Heart Association classified carotid plaques into types I–VIII based on composition. Building on this, Cai et al. introduced a modified MRI-based American Heart Association classification in 2002, which remains the most widely used carotid plaque scoring system (10). However, as this system was not specifically designed for carotid, its ability to assess plaque risk and predict cerebrovascular events is limited. To address this gap, the Plaque-RADS system was introduced in 2023 as the first standardized reporting framework dedicated to carotid plaques (11). By incorporating imaging markers such as Intraplaque Hemorrhage (IPH), Fibrous cap (FC) rupture, and intracavity thrombosis, it enables a more precise evaluation of plaque vulnerability, improving risk stratification for cerebrovascular events (12,13). Meanwhile, traditional methods for evaluating inflammation, such as measuring circulating biomarkers, lack the specificity to detect localized vascular inflammation. In this context, PFD has emerged as a valuable imaging biomarker, indirectly reflecting local inflammatory activity by quantifying changes in perivascular adipose tissue (14,15). Furthermore, studies have shown its clinical relevance as follows: Zhang et al. reported an association between PFD and IPH, while Baradaran et al. found that symptomatic patients had significantly higher mean PFD values than asymptomatic individuals (16,17). The ability to quantify perivascular inflammation offers a promising approach for predicting cerebrovascular events and may aid in the development of personalized therapeutic strategies.

The carotid plaque-RADS assesses plaque instability by incorporating imaging features such as IPH and FC rupture, while PFD serves as a noninvasive marker of local vascular inflammation. As two complementary assessment tools, their combined evaluation has the potential to overcome the

limitations of traditional stenosis-based risk assessment, offering a novel approach to stroke risk stratification. This study aims to evaluate the prognostic value of integrating Plaque-RADS and PFD in predicting stroke recurrence based on CTA and HR-VWI, providing new insights for risk stratification and personalized treatment of stroke patients.

## METHODS

### Patients

This single-center retrospective study was conducted at the our hospital, including 272 stroke patients who underwent both CTA and HR-VWI between January 2020 and December 2024 (see flowchart in Fig 1). All patients received routine treatment with single antiplatelet therapy and statins during follow-up. Inclusion criteria were as follows: (1) acute ischemic stroke confirmed by MRI upon admission; (2) carotid CTA and HR-VWI performed within two weeks of each other; and (3) plaque assessment limited to the narrowest segment of the affected carotid artery. Exclusion criteria were as follows: (1) non-atherosclerotic conditions such as dissection, aneurysm, or arteritis; (2) poor imaging quality on CTA or HR-VWI; (3) history of carotid endarterectomy or stenting; (4) presence of tumors or inflammatory lesions; and (5) comorbidities including cardiac, hepatic, or renal insufficiency. Clinical variables, including sex, age, hypertension, diabetes, and smoking history, were retrieved from the hospital information system, along with serum biomarkers such as fasting blood glucose, hemoglobin A1c, total cholesterol, triglycerides, high-density lipoprotein, and low-density lipoprotein, all collected within one week of admission.

### Scanning Parameters

HR-VWI was conducted using a Siemens MAGNETOM Prisma imaging system. The protocol included diffusion-weighted imaging, time-of-flight magnetic resonance angiography, and pre- and post-contrast 3D-T1-SPACE. The specific parameters for the 3D-T1-SPACE sequence were as follows: TR of 700 ms, TE of 15 ms, FOV of 220 mm × 220 mm, matrix size of 320 × 320, voxel dimensions of 0.3 mm × 0.3 mm × 0.7 mm, bandwidth of 504 Hz/Px, and a total acquisition time of 7 min and 16 s. Gadoteric acid (0.1 mmol/kg) was used as the contrast agent, with enhanced images acquired 10 min post-injection. The scanning procedure began with a comprehensive vascular overview of the neck.

CTA was conducted using a Siemens dual-energy CT system. The protocol included both conventional non-contrast scans and carotid CTA. Contrast was administered at an injection rate of 4.0 mL/s, with a maintenance time of 14.5 s. Imaging parameters were set as follows: slice thickness of 0.9 mm, slice spacing of 0.45 mm, pitch of 0.8625, and tube voltage of 120 kV, with an automatic adjustment of

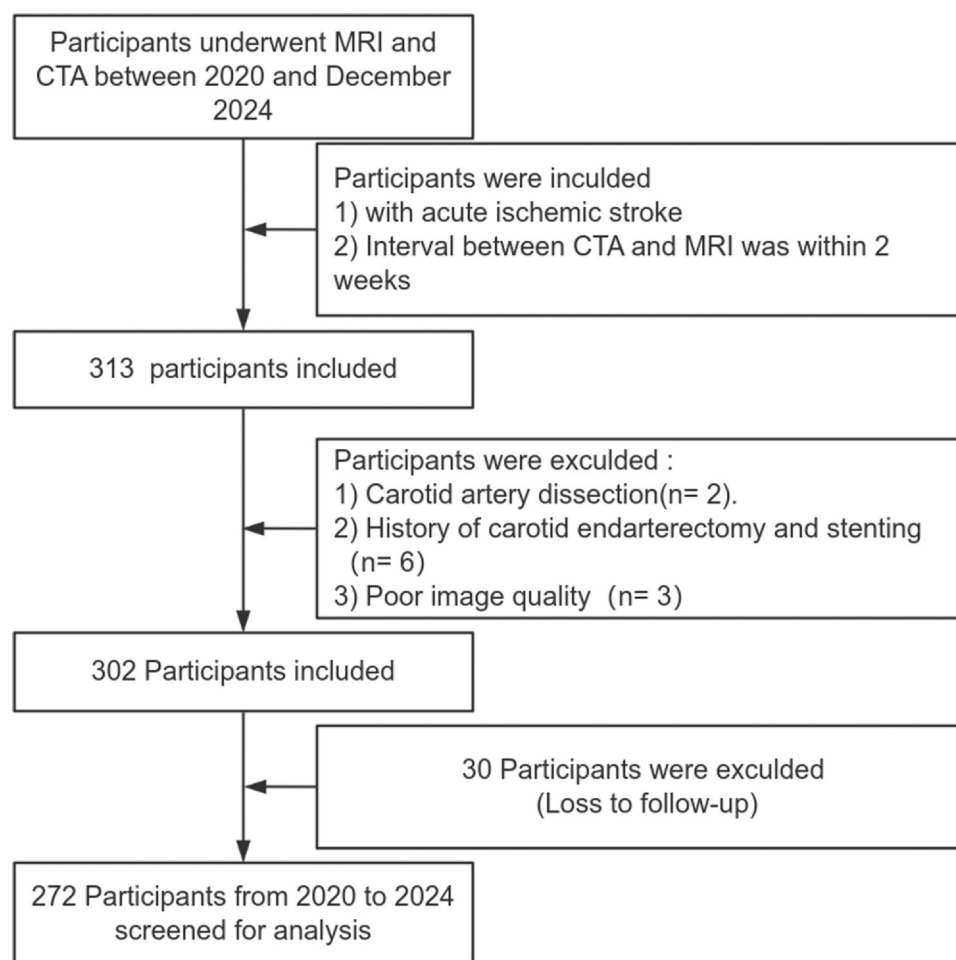


**Figure 1.** Flow chart.

current. The scan was triggered at the aortic arch when the attenuation threshold reached 100–120 HU, with image acquisition commencing 3 s thereafter. The scan range extended from the aortic arch to the skull vertex.

### Image Analysis

All HR-VWI and CTA images were independently evaluated by two radiologists with more than 5 years of experience in neuroimaging diagnosis, completely blinded to all clinical information. When the analysis results of the two radiologists were inconsistent, the final judgment was made by the superior radiologist with 10 years of experience in neuroimaging diagnosis.

### Carotid Plaque-RADS

The Carotid Plaque-RADS scores was determined based on the highest value obtained from CTA and MRI. The scores range from RADS 1 to RADS 4c (11). RADS 1 indicates a normal vessel wall without atherosclerotic plaque, while RADS 2 signifies an eccentric plaque with a maximum wall thickness (MWT) of less than 3 mm and no complex plaque characteristics. RADS 3 denotes carotid plaque with MWT

≥3 mm, potentially containing medium or large lipid-rich necrotic cores, but without complex plaque features. RADS 3 is further subdivided into three categories as follows: 3a (thick FC, MWT ≥3 mm), 3b (thin FC, MWT ≥3 mm), and 3c (ulcerative plaque, without FC rupture or intraluminal thrombosis). RADS 4 indicates the presence of at least one complex plaque feature, including IPH (4a), FC rupture (4b), or intraluminal thrombosis (4c). Because CTA cannot assess the status of the FC, RADS 3b or higher scores were derived from MRI. lipid-rich necrotic cores appear as iso-intense or slightly hyperintense on T1-weighted imaging but show no significant enhancement on contrast-enhanced T1-weighted imaging, while the adjacent FC exhibits enhancement. An ulcer is defined as a localized disruption or defect in the plaque surface that exposes the lipid core or other plaque contents to the bloodstream. Thinning of the FC is characterized by non-uniform thickness, while FC rupture is marked by a discontinuity in the FC. IPH appears as markedly hyperintense on T1-weighted imaging.

### PFD

PFD was assessed on a post-processing imaging workstation (Syngo. via, Siemens, Germany) using a predefined

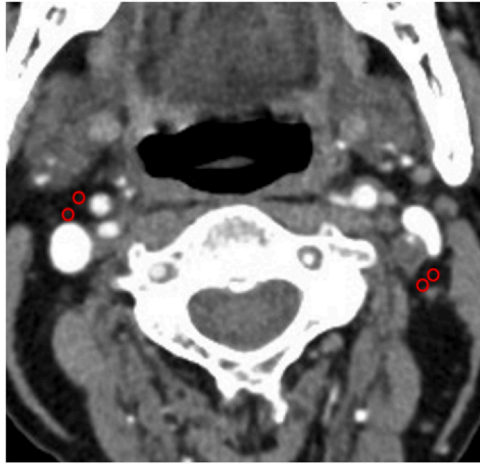


**Figure 2.** PFD measurement methods. The patient experienced an acute right-sided cerebral infarction. The red circles indicate the selected 2.5 mm<sup>2</sup> ROIs around the narrowest stenosis of the affected-side carotid artery, as well as the corresponding contralateral carotid artery at the same level.

attenuation range of  $-190$  to  $-30$  HU. Using predefined image display settings (window width: 500 HU; window level: 100 HU), we followed the analytical method described by Baradaran et al (17). For each patient, we selected an axial slice at the site of maximal luminal stenosis on the affected side. On this slice, two non-overlapping circular regions of interest (ROIs), each measuring 2.5 mm<sup>2</sup>, were manually delineated within the pericarotid fat tissue, with each ROI placed at least 1 mm away from the outer arterial wall (Fig 2). The average attenuation value of the two ROIs was defined as the affected-side PFD and reported in HU. For comparative analysis, contralateral PFD values were obtained using the same method on the same slice. Ultimately, the bilateral PFD difference was determined using the following formula: bilateral PFD difference = affected-side PFD - contralateral PFD (14). Each radiologist independently performed a complete set of measurements, including affected-side PFD, contralateral PFD, and the bilateral PFD difference. The final values used in the analysis were obtained by averaging the results from both radiologists, thereby improving measurement consistency and reliability.

### Degree of Stenosis

The degree of stenosis was categorized based on the criteria from the North American Symptomatic Carotid Endarterectomy Trial: mild stenosis (10%–29%), moderate stenosis (30%–69%), and severe stenosis (70%–99%) (18).

### CRI

As far as we know, Zhe et al. were the first to investigate the association between the Carotid Plaque-RADS and stroke recurrence risk (12). Their study identified Plaque-RADS  $\geq 3$  as an independent risk factor for stroke recurrence. Building upon these findings, we adopted the threshold proposed by

them categorizing a Plaque-RADS score  $\geq 3$  as a high-risk feature and  $< 3$  as a low-risk feature. In addition, based on the results of an independent study by Beşler et al. (19), the optimal cutoff value for PFD in predicting symptomatic patients was identified as  $-74$  HU. Given the similarity in study population characteristics, we adopted this evidence-based threshold, defining PFD  $> -74$  HU as a high-risk feature and PFD  $\leq -74$  HU as a low-risk feature. Using these two validated indicators, we developed a binary CRI combining both Plaque-RADS and PFD to offer a more robust tool for predicting stroke recurrence. Specifically, low CRI was defined as RADS  $< 3$  and PFD  $\leq -74$  HU, while high CRI was defined as RADS  $\geq 3$  or PFD  $> -74$  HU. By combining these two measures, we aim to capture both structural changes (as indicated by the Plaque-RADS) and metabolic characteristics (as indicated by PFD) of the plaque, providing a more comprehensive assessment of carotid plaque vulnerability and the risk of stroke recurrence. The effectiveness of this CRI will be validated in subsequent analyses, and its independent and incremental predictive value will be substantiated through regression analysis, ROC curve evaluation, and other methods.

### Endpoint Events

Subjects were monitored through post-stroke visit records or telephone interviews with patients or their relatives. The primary endpoint was defined as the occurrence of a recurrent stroke. Secondary endpoints included all-cause mortality. Recurrent stroke was characterized by a new focal neurological deficit lasting more than 24 h and associated with the same carotid territory as the initial stroke. Confirmation of recurrent stroke required evidence of a new acute infarction on diffusion-weighted MRI in the region corresponding to the previously identified plaque. In cases where MRI data were unavailable for patients suspected of experiencing a recurrent stroke, the nature and duration of new neurological deficits were used to confirm the event. Follow-up commenced on the date of the initial stroke diagnosis and continued until an outcome event occurred or until the study concluded in December 2024.

### Statistical Analyses

Sample size calculation and statistical analysis were performed using R software (version 4.4.1) and SPSS software (version 27.0). Data following a normal distribution were expressed as mean  $\pm$  standard deviation, while non-normally distributed data were reported as median and interquartile range. Categorical variables were summarized as frequencies or percentages. The differences in categorical variables between groups were analyzed using Chi-square tests or Fisher's exact tests, as appropriate. For continuous variables, group comparisons were made using independent t-tests or Mann-Whitney U tests, depending on the distribution. Multivariate logistic regression analysis was conducted to identify independent predictors of stroke recurrence.

Survival curves were generated using the Kaplan–Meier method, and differences were compared using the log-rank test. The Net reclassification improvement (NRI) was applied to assess the classification performance for stroke risk based on Plaque-RADS  $\geq 3$ , PFD  $> -74$  HU, and high CRI. Finally, LASSO (least absolute shrinkage and selection operator) regression was applied for variable selection and predictive model construction. To perform internal validation, a 10-fold cross-validation strategy was employed: the dataset was randomly divided into 10 equal subsets, with each subset serving as the validation set once while the remaining nine were used for training. This process was repeated 10 times, and the average area under the receiver operating characteristic curve (AUC) across the 10 iterations was calculated to evaluate the model's overall predictive performance. Decision curve analysis (DCA) was conducted to evaluate the clinical net benefit of predictive model across a range of threshold probabilities (20,21).  $P \leq 0.05$  was considered statistically significant.

## RESULT

### Characteristics of the Cohort

According to the prespecified difference in recurrence rates ( $\alpha = 0.05$ , power = 0.90, allocation ratio 1:4), the required sample size was estimated to be 40 participants. A total of 272 stroke patients were enrolled, providing sufficient power for statistical analysis. Carotid plaques were detected in 171 participants (62.9%) within the entire cohort. By December 2024, during a mean follow-up of  $17.24 \pm 11.93$  months, 64 out of 272 stroke patients (23.5%) experienced a recurrence. Detailed intergroup differences are shown in Table 1.

### Analysis of Survival

Significant differences in Kaplan–Meier survival analysis were observed across patients with Plaque-RADS of 1, 2, 3, and 4 (all  $P < 0.001$ ) (Fig 3a). The recurrence rates for each RADS score category are detailed in Table 2. When stratified by the degree of stenosis, patients with mild-to-moderate stenosis showed consistently significant differences in recurrence risk compared to those with severe stenosis ( $P < 0.001$ ) (Fig 3b). Notably, participants with mild-to-moderate carotid stenosis who were classified as high CRI or low CRI exhibited statistically significant differences in recurrent risk when compared to those classified as having mild-to-moderate stenosis alone (both  $P < 0.001$ ) (Fig 3c). These findings highlight that integrating the Plaque-RADS with PFD into a CRI can significantly improve stroke risk stratification.

### Multivariate Logistic Regression Analysis

To accurately assess the independent predictive effects of the Plaque-RADS and PFD on recurrent stroke, we controlled for potential confounders, including age, sex, and medical history. Our analysis revealed that the Plaque-RADS, CRI, affected-side PFD, bilateral PFD difference, gender, and hypertension were all significant independent predictors of recurrent stroke (Table 3).

### Incremental Prognostic Value

According to stenosis severity classification, six patients were identified as having severe stenosis and were all assigned to the high-risk group. All six experienced recurrent stroke events, indicating that this subgroup was already at extremely high risk. These patients were consistently classified as high risk by all three stratification tools—Plaque-RADS, PFD,

**TABLE 1. Baseline Characteristics of the Patients**

Variables	Non-recurrent (n = 208)	Recurrent (n = 64)	Statistic	P
Age, M (Q <sub>1</sub> , Q <sub>3</sub> )	64.00 (54.00, 74.00)	68.00 (61.50, 72.50)	Z=-1.87	0.062
Male, n(%)	153 (73.56)	37 (57.81)	$\chi^2=5.76$	<b>0.016</b>
Mild-to-moderate stenosis, n(%)	208 (100.00)	58 (90.62)	$\chi^2=15.83$	<b>&lt;.001</b>
Plaque-RADS $\geq 3$ , n(%)	32 (15.38)	38 (59.38)	$\chi^2=49.55$	<b>&lt;.001</b>
Affected-side PFD, Mean $\pm$ SD	-81.16 $\pm$ 17.64	-67.52 $\pm$ 19.33	t=-5.29	<b>&lt;.001</b>
bilateral PFD difference, Mean $\pm$ SD	5.34 $\pm$ 11.70	18.03 $\pm$ 11.56	t=-7.61	<b>&lt;.001</b>
CRI, n(%)	74 (35.58)	52 (81.25)	$\chi^2=41.06$	<b>&lt;.001</b>
Fasting blood glucose, M (Q <sub>1</sub> , Q <sub>3</sub> )	5.19 (4.34, 6.65)	5.68 (4.96, 7.02)	Z=-2.04	<b>0.042</b>
Hemoglobin A1c, M (Q <sub>1</sub> , Q <sub>3</sub> )	5.90 (5.52, 7.00)	6.10 (5.60, 7.60)	Z=-1.37	0.171
Triglycerides, M (Q <sub>1</sub> , Q <sub>3</sub> )	1.42 (1.01, 2.00)	1.46 (1.08, 1.96)	Z=-0.37	0.711
Total cholesterol, M (Q <sub>1</sub> , Q <sub>3</sub> )	4.17 (3.60, 4.86)	4.30 (3.58, 4.92)	Z=-0.13	0.894
High-density lipoprotein, M (Q <sub>1</sub> , Q <sub>3</sub> )	1.12 (0.96, 1.36)	1.17 (0.97, 1.29)	Z=-0.30	0.762
Low-density lipoprotein, M (Q <sub>1</sub> , Q <sub>3</sub> )	2.64 (2.10, 3.14)	2.75 (2.12, 3.42)	Z=-0.78	0.436
Hypertension, n(%)	139 (66.83)	52 (81.25)	$\chi^2=4.87$	<b>0.027</b>
Smoking history, n(%)	66 (31.73)	19 (29.69)	$\chi^2=0.10$	0.758
Drinking history, n(%)	54 (25.96)	17 (26.56)	$\chi^2=0.01$	0.924

Values in bold indicate  $P < 0.05$ . CRI, comprehensive risk index; M, mean; PFD, pericarotid fat density; Q<sub>1</sub>, First Quartile, 25th Percentile; Q<sub>3</sub>, Third Quartile, 75th Percentile; RADS, reporting and data system; SD, standard deviation.



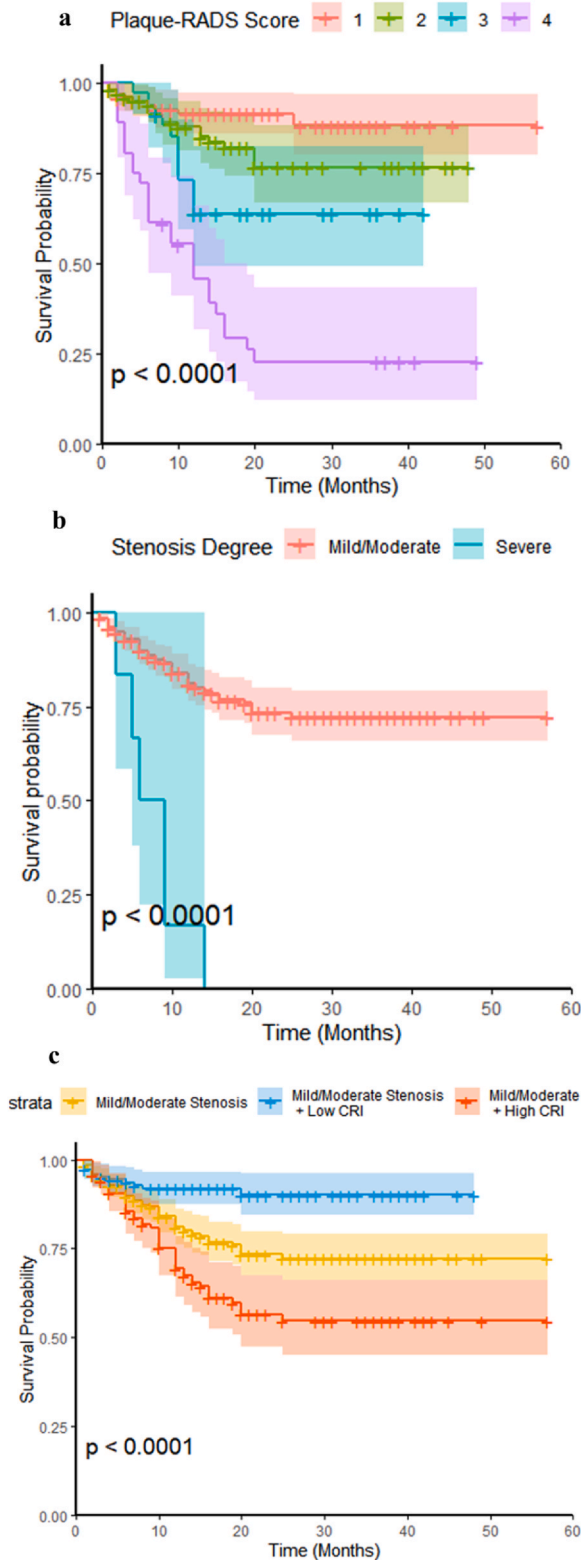


**Figure 3.** Kaplan-Meier survival analysis. **(a)** KM survival curves stratified by Plaque-RADS. As the Plaque-RADS increases, the stroke recurrence rate significantly decreases. **(b)** KM survival curves stratified by the degree of stenosis. **(c)** KM survival curves stratified by degree of stenosis and CRI. The CRI demonstrated better risk stratification ability in subjects with mild-to-moderate carotid stenosis. The recurrence rate of high CRI and low CRI patients with mild-to-moderate stenosis showed significant differences compared to mild-to-moderate stenosis patients who were not stratified.

**TABLE 2. Specific Distribution of Carotid Plaque-RADS**

Plaque-RADS	Non-recurrent (n = 208)	Recurrent (n = 64)
RADS 1	92(44.23)	9(14.06)
RADS 2	84(40.38)	17(26.56)
RADS 3	22(10.58)	12(18.75)
3a	9	2
3b	6	8
3c	7	2
RADS 4	10(4.81)	26(40.63)
4a	6	12
4b	3	8
4c	1	6

RADS, reporting and data system.

and CRI. As a result, these tools offered no additional discriminatory value in this subgroup. The incremental predictive value relative to stenosis classification was therefore primarily demonstrated in patients with mild-to-moderate stenosis. The stroke recurrence rate was 21.8% in patients with mild-to-moderate stenosis, 11.8% in those with low CRI, and 41.1% in those with high CRI for mild-to-moderate stenosis. This trend highlights the importance of reclassifying stenosis severity using Plaque-RADS and PFD. CRI combining Plaque-RADS and PFD significantly improved the accuracy of stroke risk reclassification in patients with mild-to-moderate stenosis. Among 58 patients with mild-to-moderate stenosis (n = 58), 46 (79.3%) were accurately reclassified as high-risk by the CRI assessment. The NRI index was 36.30% (Fig 4).

### ROC and DCA Curve Analysis

To assess the CRI on stroke recurrence and mitigate potential multicollinearity between Plaque-RADS and PFD, we employed the Lasso regression model. Figure 5a presents the ROC curve analysis, demonstrating that as model complexity increased, the AUC value also improved. Specifically, Model 1 yielded an AUC of 0.719, whereas Model

TABLE 3. Multivariate Logistic Regression Analysis on Recurrent Stroke

Variables	$\beta$	S.E	Z	P	OR (95%CI)
Age	0.02	0.02	1.17	0.241	1.02 (0.99 ~ 1.05)
Male	-1.53	0.47	-3.26	<b>0.001</b>	0.22 (0.09 ~ 0.54)
degree of stenosis	16.94	923.54	0.02	0.985	-
Plaque-RADS $\geq 3$	0.99	0.49	2.03	<b>0.042</b>	2.68 (1.03 ~ 6.96)
Affected-side PFD	-0.03	0.01	-2.27	<b>0.023</b>	0.97 (0.94 ~ 0.99)
Bilateral PFD difference	0.09	0.02	4.44	<b>&lt; .001</b>	1.09 (1.05 ~ 1.13)
CRI	2.11	0.67	3.17	<b>0.002</b>	8.25 (2.23 ~ 30.44)
Fasting blood glucose	-0.04	0.10	-0.39	0.696	0.96 (0.78 ~ 1.18)
Hemoglobin A1c	-0.06	0.15	-0.37	0.710	0.94 (0.70 ~ 1.28)
Triglycerides	0.04	0.17	0.24	0.807	1.04 (0.75 ~ 1.46)
Total cholesterol	-0.64	0.43	-1.51	0.131	0.52 (0.23 ~ 1.21)
High-density lipoprotein	-0.76	0.67	-1.14	0.252	0.47 (0.13 ~ 1.72)
Low-density lipoprotein	0.90	0.50	1.78	0.075	2.45 (0.91 ~ 6.57)
Hypertension	1.10	0.46	2.36	<b>0.018</b>	2.99 (1.20 ~ 7.43)
Smoking history	0.29	0.48	0.60	0.549	1.33 (0.52 ~ 3.42)
Drinking history	0.79	0.54	1.46	0.145	2.21 (0.76 ~ 6.41)

Values in bold indicate  $P < 0.05$ . CI, confidence interval; CRI, comprehensive risk index; OR, odds ratio; PFD, pericarotid fat density; RADS, reporting and data system

5 achieved an AUC of 0.892, highlighting the significant enhancement in predictive performance when incorporating comprehensive risk indicators (Table 4). The prediction of stroke recurrence based exclusively on the degree of carotid stenosis has inherent limitations. The DCA (Fig 5b) further confirms that incorporating the Plaque-RADS and PFD significantly enhances the predictive accuracy for stroke recurrence risk. Notably, Model 5, which integrates the Plaque-RADS, PFD, and CRI, provides substantial net benefits at lower risk thresholds (0.1–0.5).

## DISCUSSION

Ischemic stroke has a high recurrence rate and significantly increases the risk of death and disability, with the latter being 9.4 times higher after a recurrent event compared to an initial stroke (22). Although secondary prevention strategies have been shown to effectively reduce recurrence risk, reliable methods for predicting stroke recurrence remain limited. Traditional risk assessment of carotid plaques has predominantly relied on the degree of stenosis. The latest guidelines from the European Society for Vascular Surgery (2023) (23) and the Society for Vascular Surgery (2022) (24) continue to recommend a 50% stenosis threshold as the criterion for surgical intervention in symptomatic patients. However, growing evidence suggests that stenosis severity alone may not accurately reflect the true risk conferred by atherosclerotic plaques, particularly in individuals with mild-to-moderate stenosis or even no carotid stenosis (25). In these populations, plaques with high-risk features—such as IPH, FC rupture, or intraluminal thrombus—despite lacking severe stenosis, have been strongly associated with stroke recurrence (26,27).

The carotid Plaque-RADS score, a standardized multi-modal imaging assessment system, offers a systematic quantification of plaque structural integrity and vulnerability, providing a promising direction for enhancing stroke risk prediction. Prior studies have validated its predictive utility: for instance, Song et al. (28) demonstrated that the Plaque-RADS effectively identified individuals at high risk of new-onset stroke, while Huang et al. (12) further confirmed its value in assessing recurrence risk. Building on this foundation, the present study extends the Plaque-RADS framework by incorporating PFD—a marker of local vascular inflammation—into a novel CRI that integrates both structural and functional dimensions of plaque biology. PFD, a quantitative parameter derived from CTA, reflects inflammatory crosstalk between the vessel wall and surrounding adipose tissue. Its elevation has been shown to correlate with plaque instability in coronary artery disease and has recently been applied in carotid atherosclerosis research (29–31). In contrast to RADS, which emphasizes anatomical assessment, PFD captures dynamic inflammatory activity, thereby complementing structural metrics and addressing the limitations of morphology-based risk stratification (32,33).

The CRI is supported by a robust biological rationale and demonstrates high feasibility and predictive value in clinical practice. Our findings show that both the Plaque-RADS and PFD serve as independent predictors of stroke recurrence. When combined into the CRI, their integration significantly improves risk stratification performance. Notably, among patients with mild-to-moderate stenosis—traditionally regarded as having a low intervention priority—those with high CRI scores exhibited a markedly increased risk of recurrence, highlighting a potential underestimation of risk when relying solely on conventional stenosis-based classifications. Based on the joint assessment of CRI and stenosis

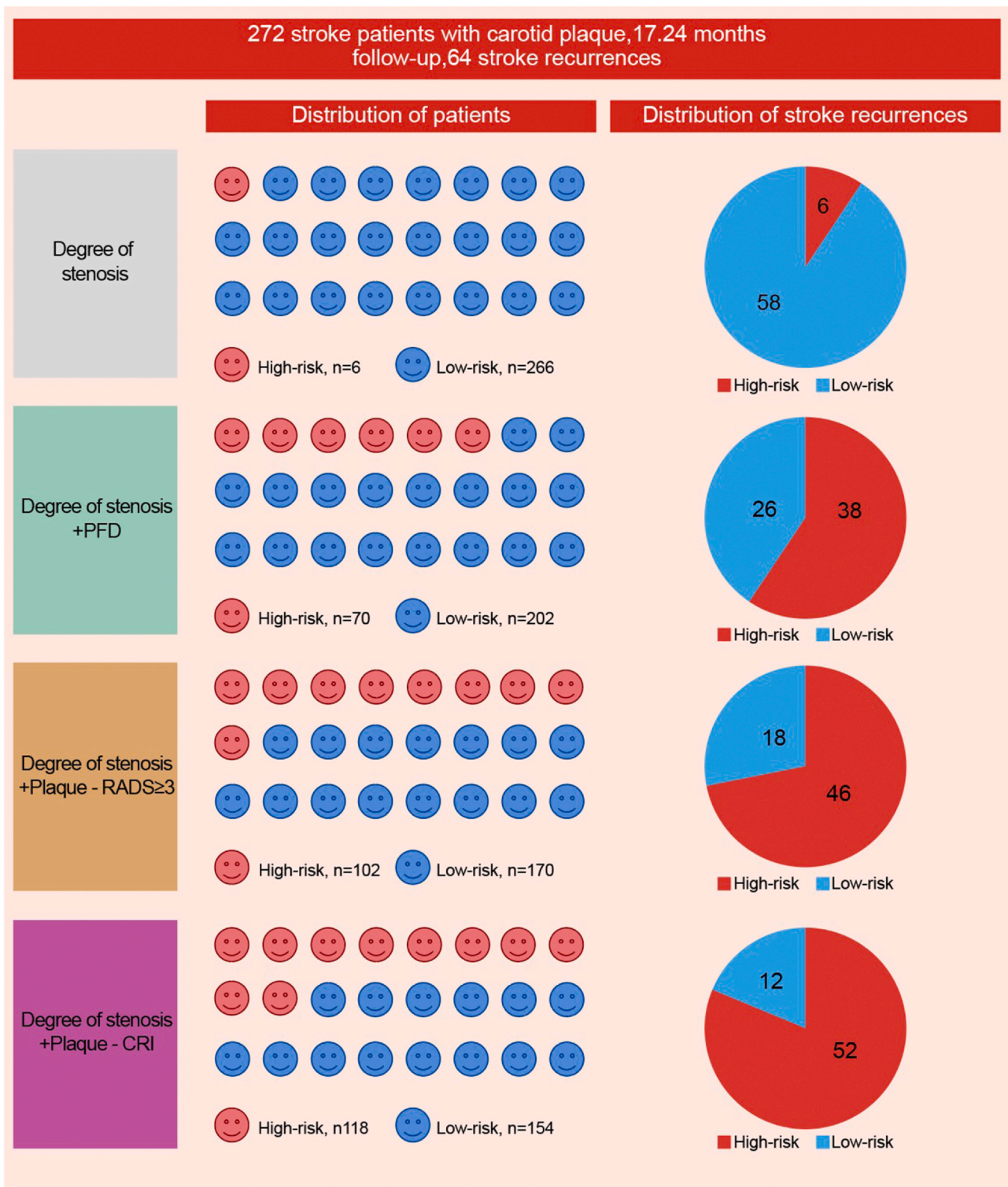


**Figure 4.** Under the classification based on the degree of stenosis, 58 stroke patients were categorized as having mild-to-moderate stenosis. Among these 58 patients with mild-to-moderate stenosis, 32 patients with PFD  $> -74$  HU were correctly reclassified, with an NRI of 29.81%. Under the classification based on RADS score  $\geq 3$ , 40 patients were reclassified, with an NRI of 34.62%. Finally, under the comprehensive risk index classification, 46 out of the 58 mild-to-moderate stenosis patients were correctly reclassified as having a high comprehensive risk index, with an NRI of 36.3%. Low CRI: RADS  $< 3$  and PFD  $< -74$  HU; high CRI: RADS  $\geq 3$  or PFD  $> -74$  HU. CRI, comprehensive risk index; NRI, net classification indices; PFD, pericarotid fat density; RADS, reporting and data system.



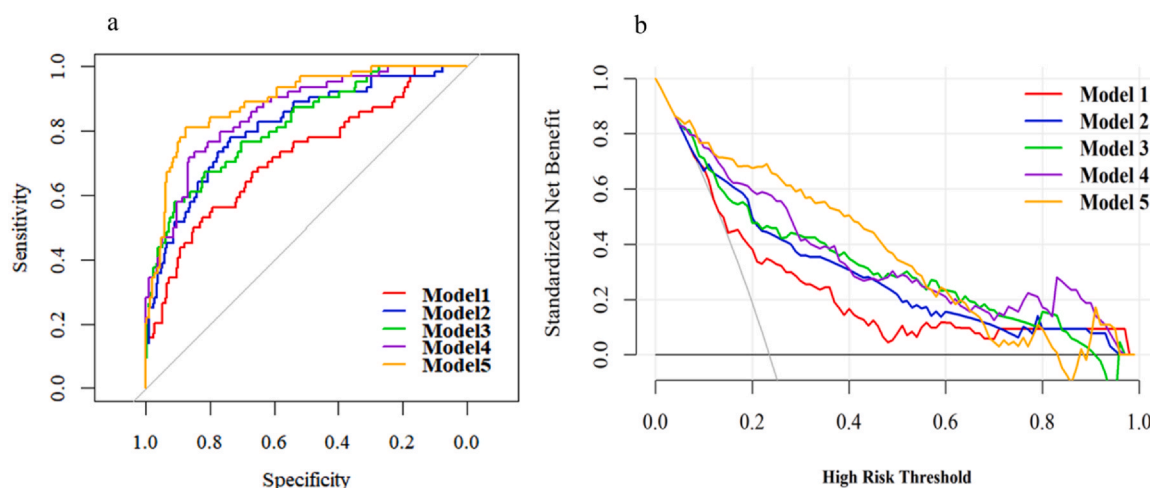


**Figure 5.** ROC curves. (a) ROC curves. (b) DCA curves. Model 1 includes the conventional degree of stenosis. Model 2 builds on Model 1 by incorporating the Plaque-RADS. Model 3 builds on Model 1 by adding the PFD. Model 4 extends Model 1 by integrating both the Plaque-RADS and PFD. Model 5 further expands Model 4 by including the CRI. (In the model, PFD includes affected-side PFD and bilateral PFD difference). DCA, decision curve analysis; ROC, receiver operating characteristic.

severity, 17.29% of patients with a prior stroke (46 out of 266) were correctly reclassified into a more appropriate risk category, yielding an NRI of 36.30%. These results underscore the incremental predictive value of CRI, which enhances risk identification by integrating both plaque structural vulnerability and localized inflammatory activity.

However, the potential for misclassification remains an inherent limitation in the real-world application of CRI. In our cohort, the false-negative rate was 5.3% (12 out of 266), and the false-positive rate reached 29.2% (66 out of 266). False negatives may lead to an underestimation of risk and insufficient follow-up or preventive measures, whereas false positives could result in overestimation of risk, unnecessary diagnostic testing, intensified treatment, and increased psychological burden. Therefore, although CRI demonstrates favorable overall predictive accuracy, its application should be complemented by individualized clinical evaluation—particularly for patients at borderline risk—to achieve a more balanced approach between predictive sensitivity and resource utilization efficiency.

Further joint modeling analyses confirmed the superior performance of the proposed tool. Model 4, which

integrated the Plaque-RADS and the PFD, demonstrated improved predictive power for stroke recurrence compared to either marker used individually, highlighting the strong complementarity between structural vulnerability and inflammatory activity. Upon incorporating the CRI into Model, model 5 performance improved further, with the AUC rising from 0.858 to 0.892, indicating enhanced risk discrimination. DCA revealed that Model 5 consistently provided greater net clinical benefit across a range of decision thresholds, particularly in the low-risk range (0.1–0.5), supporting its utility in early screening and individualized management strategies for broader populations. From a mechanistic perspective, stroke recurrence is not driven by a single pathological factor but rather reflects the combined impact of plaque structural disruption and local vascular inflammation. Experimental studies have shown that stroke events can activate the AIM2 inflammasome within carotid plaques, intensifying local inflammatory responses and compromising plaque stability (34). This contributes to a self-reinforcing pathological cycle of “stroke induction → inflammation aggravation → plaque destabilization → stroke recurrence”. By integrating the structural fragility captured

**TABLE 4.** Area Under the Receiver Operating Characteristic Curve of the Prediction Model

Model	AUC	Accuracy	Sensitivity	Specificity	P
Model1	0.719	0.790	0.125	0.995	
Model2	0.814	0.805	0.266	0.971	0.014
Model3	0.817	0.820	0.297	0.981	0.015
Model4	0.858	0.831	0.422	0.957	0.001
Model5	0.892	0.846	0.531	0.942	0.000

Model 1 includes the conventional degree of stenosis. Model 2 builds on Model 1 by incorporating the Plaque-RADS. Model 3 builds on Model 1 by adding the PFD. Model 4 extends Model 1 by integrating both the Plaque-RADS and PFD. Model 5 further expands Model 4 by including the CRI. (In the model, PFD includes affected-side PFD and bilateral PFD difference)

by Plaque-RADS and the inflammatory activity indicated by PFD, the CRI provides a multi-dimensional assessment of stroke recurrence risk and more comprehensively reflects its core pathophysiological mechanisms. As such, CRI holds promise as a clinically actionable tool for early identification and stratification of high-risk patients, and may inform the development of more refined, individualized secondary prevention strategies.

In this study, we proposed an innovative approach by integrating the Plaque-RADS with PFD to construct a CRI for predicting stroke recurrence. While this approach holds significant exploratory value, several limitations should be acknowledged. First, the study was conducted as a single-center retrospective analysis, and the generalizability of the findings requires further validation using larger, multicenter datasets. Second, model performance was evaluated solely through 10-fold cross-validation within the same dataset, without the inclusion of an independent external test set. Although cross-validation is a widely accepted internal validation method, its reliance on data partitions from the original cohort may introduce potential biases and limit the model's ability to generalize to truly independent populations. Finally, despite the strong theoretical rationale supporting the CRI, its definition and measurement methodology require further standardization to enhance reproducibility and facilitate broader clinical implementation.

## CONCLUSION

This study demonstrates that incorporating carotid Plaque-RADS and PFD into a CRI significantly improves the accuracy of stroke recurrence risk prediction compared to using stenosis severity alone. By integrating plaque structural characteristics with local inflammatory markers, the CRI outperforms individual metrics in identifying high-risk patients, particularly among those with mild-to-moderate stenosis where conventional grading often lacks discriminatory power. These findings underscore the clinical value of the CRI in enhancing risk stratification and highlight its potential to inform more precise and personalized secondary prevention strategies.

## FUNDING INFORMATION

This work was supported by Nantong Municipal Health Commission (MS2023033) and Clinical Medicine Specialized Project of Nantong University (2022LQ004).

## AUTHOR CONTRIBUTION

JQ and QC drafted the manuscript. JQ, QC, and TZ were responsible for data collection. QC and CQ performed the statistical analysis. RY and LZ contributed to the study

design. WD, ZC, and TW participated in data review and manuscript revision.

## DECLARATION OF COMPETING INTEREST

All the authors declare that they have no conflicts of interest related to this work.

## REFERENCES

- Li J, Zhang Y, Hou J, et al. Clinical application of dark-blood imaging in head and neck CT angiography: effect on image quality and plaque visibility. *Acad Radiol* 2024; 31:2478–2487.
- Mohan KM, Wolfe CD, Rudd AG, et al. Risk and cumulative risk of stroke recurrence: a systematic review and meta-analysis. *Stroke* 2011; 42(5):1489–1494.
- Flach C, Muruet W, Wolfe C, et al. Risk and secondary prevention of stroke recurrence: a population-base cohort study. *Stroke* 2020; 51(8):2435–2444.
- Rothwell PM, Eliasziw M, Gutnikov SA, et al. Analysis of pooled data from the randomised controlled trials of endarterectomy for symptomatic carotid stenosis. *Lancet* 2003; 361(9352):107–116.
- Capoccia L, Sirignano P, Mansour W, et al. Peri-procedural brain lesions prevention in CAS (3PCAS): randomized trial comparing CGuard™ stent vs. Wallstent™. *Int J Cardiol* 2019; 279:148–153.
- Huang Q, Liu L, Zhang S, et al. Characteristics of atherosclerotic plaques and stroke mechanism in patients with border-zone infarcts: a high-resolution magnetic resonance imaging study. *Acad Radiol* 2024; 31:3929–3943.
- Kamtchum-Tatuene J, Saba L, Heldner MR, et al. Interleukin-6 predicts carotid plaque severity, vulnerability, and progression. *Circ Res* 2022; 131(2):e22–e33.
- Liu Y, Zhao Y, Guo Z, et al. A novel predictive model based on pericarotid adipose tissue and lumen stenosis for stroke risk in patients with asymptomatic carotid stenosis. *J Investig Med* 2024; 72(3):270–278.
- Zietz A, Gorey S, Kelly PJ, et al. Targeting inflammation to reduce recurrent stroke. *Int J Stroke* 2024; 19(4):379–387.
- Cai JM, Hatsukami TS, Ferguson MS, et al. Classification of human carotid atherosclerotic lesions with in vivo multicontrast magnetic resonance imaging. *Circulation* 2002; 106(11):1368–1373.
- Saba L, Cau R, Murgia A, et al. Carotid plaque-RADS: a novel stroke risk classification system. *JACC Cardiovasc Imaging* 2024; 17(1):62–75.
- Huang Z, Cheng XQ, Lu RR, et al. Incremental prognostic value of carotid plaque-RADS over stenosis degree in relation to stroke risk. *JACC Cardiovasc Imaging* 2024. S1936-878X(24)00290-0 [pii].
- Xia J, Yu C, Li L, et al. Arterial transit artifacts and carotid Plaque-RADS may predict symptoms in patients with carotid stenosis. *Magn Reson Imaging* 2024; 111:131–137.
- Yu M, Meng Y, Zhang H, et al. Associations between pericarotid fat density and image-based risk characteristics of carotid plaque. *Eur J Radiol* 2022; 153:110364.
- Cau R, Anzalone N, Mannelli L, et al. Pericarotid fat as a marker of cerebrovascular risk. *AJNR Am J Neuroradiol* 2024; 45(11):1635–1641.
- Zhang S, Yu X, Gu H, et al. Identification of high-risk carotid plaque by using carotid perivascular fat density on computed tomography angiography. *Eur J Radiol* 2022; 150:110269.
- Baradaran H, Myneni PK, Patel P, et al. Association between carotid artery perivascular fat density and cerebrovascular ischemic events. *J Am Heart Assoc* 2018; 7:e010383.
- Ferguson GG, Eliasziw M, Barr HW, et al. The North American symptomatic carotid endarterectomy trial: surgical results in 1415 patients. *Stroke* 1999; 30(9):1751–1758.
- Beşler MS, Karadenizli MB, Ökten RS. A novel imaging biomarker for prediction of cerebrovascular ischemic events: pericarotid fat density. *Am J Emerg Med* 2024; 84:130–134.
- Vickers AJ, Elkin EB. Decision curve analysis: a novel method for evaluating prediction models. *Med Decis Making* 2006; 26:565–574.
- Vickers AJ, van Calster B, Steyerberg EW. A simple, step-by-step guide to interpreting decision curve analysis. *Diagn Progn Res* 2019; 3:18.
- Kang K, Park TH, Kim N, et al. Recurrent stroke, myocardial infarction, and major vascular events during the first year after acute ischemic stroke: the multicenter prospective observational study about

- recurrence and its determinants after acute ischemic stroke I. *J Stroke Cerebrovasc Dis* 2016; 25(3):656–664.
23. Naylor R, Rantner B, Ancetti S, et al. Editor's Choice - European Society for Vascular Surgery (ESVS) 2023 Clinical Practice Guidelines on the management of atherosclerotic carotid and vertebral artery disease. *Eur J Vasc Endovasc Surg* 2023; 65(1):7–111.
  24. AbuRahma A. An analysis of the recommendations of the 2022 Society for Vascular Surgery Clinical Practice Guidelines for Patients with Asymptomatic Carotid Stenosis. *J Vasc Surg* 2024; 79:1235–1239.
  25. Hu D, Yu L, Feng B, et al. Acute moderate hemodynamic stroke secondary to large vessel stenosis: a case series exploring imaging characteristics and endovascular treatment outcomes. *Acad Radiol* 2025. S1076-6332(25)00096-0, Online ahead of print.
  26. Huang Z, Cheng XQ, Lu RR, et al. A radiomics-based nomogram using ultrasound carotid plaque evaluation for predicting cerebro-cardiovascular events in asymptomatic patients. *Acad Radiol* 2024; 31:5204–5216.
  27. Kopczak A, Schindler A, Bayer-Karpinska A, et al. Complicated carotid artery plaques as a cause of cryptogenic stroke. *J Am Coll Cardiol* 2020; 76(19):2212–2222.
  28. Song JW, Phi HQ, Koneru M, et al. Prevalence of high-risk CTA-based carotid plaque-RADS subtypes in patients with embolic stroke of undetermined source. *Stroke* 2025; 56:737–740.
  29. Goeller M, Achenbach S, Cadet S, et al. Pericoronary adipose tissue computed tomography attenuation and high-risk plaque characteristics in acute coronary syndrome compared with stable coronary artery disease. *JAMA Cardiol* 2018; 3(9):858–863.
  30. Stanek A, Brożyna-Tkaczyk K, Myśliński W. The role of obesity-induced perivascular adipose tissue (PVAT) dysfunction in vascular homeostasis. *Nutrients* 2021; 13(11):3843.
  31. Saba L, Zucca S, Gupta A, et al. Perivascular fat density and contrast plaque enhancement: does a correlation exist. *AJNR Am J Neuroradiol* 2020; 41(8):1460–1465.
  32. Zhang A, Ren M, Deng W, et al. Ischemia in intracerebral hemorrhage: a comparative study of small-vessel and large-vessel diseases. *Ann Clin Transl Neurol* 2022; 9:79–90.
  33. Lin A, Dey D, Wong D, et al. Perivascular adipose tissue and coronary atherosclerosis: from biology to imaging phenotyping. *Curr Atheroscler Rep* 2019; 21(12):47.
  34. Cao J, Roth S, Zhang S, et al. DNA-sensing inflammasomes cause recurrent atherosclerotic stroke. *Nature* 2024; 633(8029):433–441.